

Interdependence of Magnetism and Superconductivity in the Borocarbide $\text{TmNi}_2\text{B}_2\text{C}$

K.N. Røsgaard, M.R. Eskildsen and N.H. Andersen

Condensed Matter Physics and Chemistry Department, Risø National Laboratory, DK-4000 Roskilde, Denmark

J. Jensen, P. Hedegård and S.N. Kjausén

Røst Laboratory, Niels Bohr Institute (APG), Universitetsparken 5, DK-2100 Copenhagen, Denmark

P.C. Canfield

Ames Laboratory and Department of Physics and Astronomy, Iowa State University, Ames, Iowa 50011
(December 14, 1999)

We have discovered a new antiferromagnetic phase in $\text{TmNi}_2\text{B}_2\text{C}$ by neutron diffraction. The ordering vector is $Q_A = (0.48; 0; 0)$ and the phase appears above a critical in-plane magnetic field of 0.9 T. The field was applied in order to test the assumption that the zero-field magnetic structure at $Q_F = (0.094; 0.094; 0)$ would change into a c-axis ferromagnet if superconductivity were destroyed. We present theoretical calculations which show that two effects are important: A suppression of the ferromagnetic component of the RKKY exchange interaction in the superconducting phase, and a reduction of the superconducting condensation energy due to the periodic modulation of the moments at the wave vector Q_A .

PACS numbers: 74.70.Dd, 75.25.+z, 74.20.Fg

The interplay between magnetism and superconductivity is inherently of great interest since the two phenomena represent ordered states which are mutually exclusive in most systems. Therefore, the borocarbide intermetallic quaternaries with stoichiometry $(\text{RE})\text{Ni}_2\text{B}_2\text{C}$ have attracted great attention since the publication of their discovery in 1994 [1,2], as they exhibit coexistence of magnetism and superconductivity if the rare earth (RE) is either Dy, Ho, Er or Tm. The magnetic moments in these compounds are due to the localized 4f electrons of the rare-earth ions. The 4f and the itinerant electrons are coupled weakly by the exchange interaction, resulting in the indirect Ruderman-Kittel-Kasuya-Yoshida (RKKY) interaction between the 4f-moments. Thus the RKKY interaction, which is decisive for the cooperative behavior of the magnetic electrons, depends on the state of the metallic ones.

The borocarbides have a tetragonal crystal structure with space group $(I4/mmm)$ [3], and $\text{TmNi}_2\text{B}_2\text{C}$ has a superconducting critical temperature $T_c = 11$ K and a Neel temperature $T_N = 1.5$ K [4]. The crystalline electric field aligns the thulium moments along the c axis, and the magnetic structure has a short fundamental ordering vector $Q_F = (0.094; 0.094; 0)$ with several higher-order odd harmonics [5,6]. In the magnetic structures detected in any of the other systems, the moments of the rare-earth ions are confined to the basal plane, and they have short wavelength antiferromagnetically ordered states. For example, they are commensurate with a propagation vector $Q = (0; 0; 1)$ for RE = Ho and Dy, or incommensurate with $Q = (0.55; 0; 0)$ for RE = Gd, Tb, Ho and Er [5]. An especially tight coupling between magnetism and superconductivity has been clearly demonstrated in

$\text{TmNi}_2\text{B}_2\text{C}$, where a magnetic field applied along the c axis induced concurrent changes of the magnetic structure and the symmetry of the flux line lattice [7]. Similar effects have not yet been observed in any of the other borocarbides.

One question that immediately arises, and which we believe is important for the general understanding of the interaction between superconductivity and magnetism, is why the long-period magnetic ordering found in $\text{TmNi}_2\text{B}_2\text{C}$ is stable. Band structure calculations on the normal state of non-magnetic $\text{LuNi}_2\text{B}_2\text{C}$ predict a maximum in the conduction-electron susceptibility (q) at $q = (0.6; 0; 0)$ supported by Fermi-surface nesting [8,9]. The RKKY interaction is proportional to the magnetic susceptibility of the electron gas, and the position of its maximum, determining the magnetic ordering vector, is expected to be nearly the same as in (q). This is in agreement with the experimental findings for many of the magnetic borocarbides, but not for $\text{TmNi}_2\text{B}_2\text{C}$.

The use of the band structure of the normal state ignores that the magnetic interactions are mediated by a superconducting medium. The BCS ground state is a singlet and apart from the interband scattering the electronic susceptibility is therefore zero at $q = 0$ and zero temperature. It will recover its normal-state value only when $q > 10^{-1}$, where λ is the coherence length of the superconductor, as first pointed out by Anderson and Suhl [10]. This raises the possibility that a local maximum in the susceptibility is shifted from zero in the normal phase to a non-zero value of q in the superconducting phase. In the case of the free electron gas, this maximum is very shallow and occurs at a relatively large q . If, however, interband effects (or umklapp processes in the free

electron model) are included the situation is changed. We shall write the RKKY interaction in the superconducting phase as $J(q) = I[\chi_0(q) + \chi_u(q)]$. $\chi_0(q)$ is the contribution from the intraband scattering near the Fermi surface, which is sensitive to the superconducting energy gap. We have determined this function numerically in the zero temperature limit by using a linear expansion in q of the band electron energies near the Fermi surface. A simple fit to the result is $\chi_0(q) = 0.99q[q + 1.5^{-1}]^{-1}\chi_0(0)$, where $\xi = (\hbar v_F)$ is the coherence length. The superconducting energy gap is negligible compared to the band splittings, and the contribution $\chi_u(q)$ from the interband scattering is therefore not affected by the state of the conduction electrons. At small q we may assume: $\chi_u(q) = \chi_0(0)(Aq^2)$, where A is a constant normal-state quantity, which is expected to be some few times $(2/a)^2$, where a is the lattice parameter. The local maximum in $J(q)$, at $q = 0$ in the normal phase, will in the superconducting phase appear at $q_0 = [(4/3)A]^{1/3}$. This is the same dependence on ξ as found by Anderson and Suhl, but the coefficient does not depend explicitly on k_F and is somewhat smaller. With $A(2/a)^2$ lying between 1 and 10, q_0 assumes a value between 0.084 and 0.18 times $2/a$, which is consistent with the magnitude of the observed ordering vector, $Q_F = 0.13(2/a)$.

The existence of a local maximum in the RKKY interaction is not sufficient for stabilizing a magnetic structure with that wavelength. The total free energy of the entire system, including the condensation energy of the superconducting electrons, has to be minimal. The presence of a magnetic modulation at Q may in principle weaken the superconductivity, for instance through a reduction of the density of states at the Fermi surface due to the superzone energy gaps created by the periodic modulation of the moments. This effect depends strongly on Q and may be an important factor in the competition between alternative magnetic structures.

In this letter we report the results of neutron diffraction studies on $TmNi_2B_2C$ augmented by theoretical calculations of the competition between the magnetic and superconducting states. With the objective of suppressing superconductivity while the c -axis components of the magnetic moments are still ordered, a magnetic field was applied in the basal plane. This allows a study of the magnetic state as it would be in the absence of superconductivity. The experimental results are described in detail below. Briefly we found that the system does not form a ferromagnetic state when superconductivity is suppressed, as one might expect from the arguments presented above, but instead it relaxes into an incommensurate antiferromagnetic state with $Q = Q_A = (0.482; 0; 0)$, resembling the magnetic ordering most commonly found in the borocarbides.

The experiments were performed on a $2 \times 2 \times 0.2$ mm³ single crystal of $TmNi_2B_2C$ grown by a high-temperature flux method and isotopically enriched with ¹¹B to en-

hance the neutron transmission [11,12]. The sample was mounted on a copper rod in a dilution refrigerator insert for the low-temperature measurements at $T < 1.7$ K, and on a standard sample stick for measurements above 1.7 K. In both cases the sample was oriented with the a - and b -axes in the scattering plane and placed in a 1.8 T horizontal field magnet aligned along the a axis. Measurements were performed with applied fields up to the maximum of 1.8 T, and at temperatures between 20 mK and 6 K. The neutron diffraction experiments were performed at the TAS7 triple-axis spectrometer on the cold neutron beam line at the DR3 research reactor at Risø National Laboratory. The measurements were carried out with 12.75 meV neutrons, pyrolytic graphite (004) monochromator and (002) analyzer crystals, and in an open geometry without collimation. The effective beam divergence before and after the sample was 60 and 120 arc minutes, respectively.

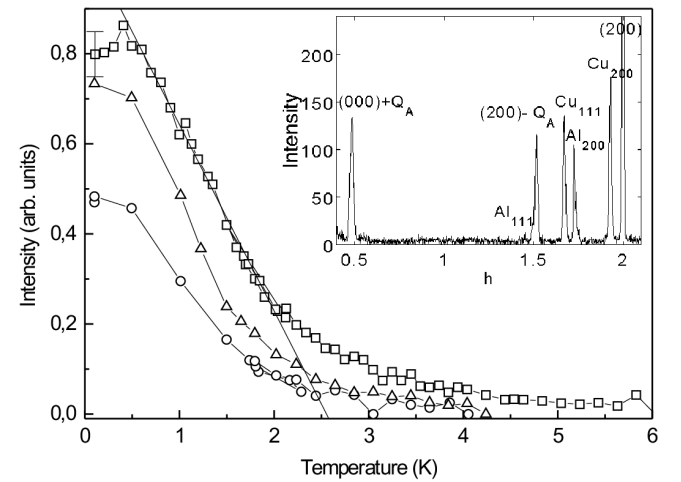


Fig. 1 Normalized integrated intensities versus temperature of the field-induced magnetic peaks at 1.2 T (circles), 1.4 T (triangles) and 1.8 T (squares). The linear fit to the 1.8 T data shows the determination of $T_N(B)$. Inset: Scan along the $[100]$ direction at $T = 100$ mK and 1.8 T, showing the field-induced satellite peaks at $Q_A = (0.482; 0; 0)$ around the (000) and (200) nuclear reflections. The peak intensity of the (200) reflection is 800.

In the inset to Fig. 1 is shown the result of a scan along $[100]$ at $T = 100$ mK and $B = 1.8$ T. In addition to the nuclear (200) Bragg reflection, the figure shows satellite peaks at $(000) + Q_A$ and $(200) - Q_A$ with $Q_A = (0.482; 0; 0)$. These satellite peaks are not observed in zero applied field neither below nor above T_N , and they do not appear until the field is larger than 0.9 T at 100 mK. Additional magnetic satellites were detected at $(110) - Q_A$ and $(020) - Q_A$. No higher order harmonics of the field-induced satellites were observed, and their intensities are consistent with the magnitude and direction of the magnetic moments remaining equal to $3.8 \mu_B$ and being essentially parallel to the c axis. At all temperatures and fields, where the Q_A peaks were observed, they stayed resolution limited. Likewise no field

or temperature dependence of Q_A was found. Quite remarkably, the field-induced peaks are only observed for the wave vector Q_A k B and not for Q_A ? B, hence the lowering of the in-plane four-fold symmetry of the system produced by the field has a direct consequence on the direction of Q_A .

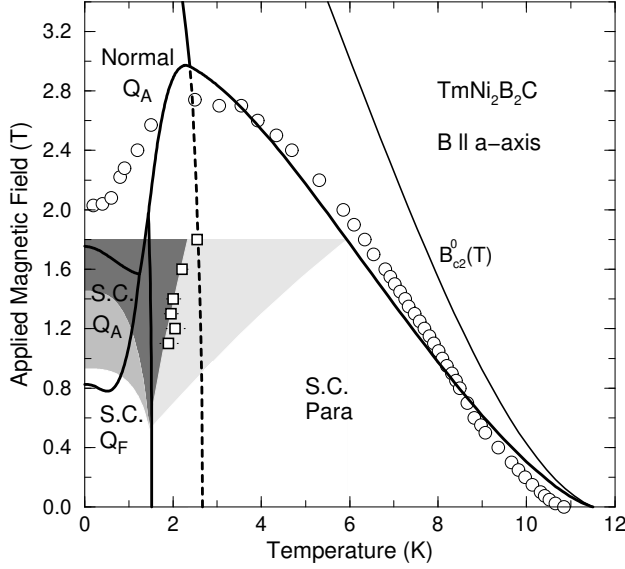


Fig. 2 Experimental and theoretical phase diagram of $TmNi_2B_2C$ in a magnetic field along $[100]$. The medium-gray area denotes the region where both the Q_A and the Q_F reflections are present. In the dark-gray area only the Q_A reflections were observed, up to the maximum applied field of 1.8 T. The light-gray area denotes the region where the long tail of low-intensity magnetic scattering at Q_A is still observed. The squares denote the measured phase boundary between the Q_A phase and the paramagnetic one, $T_N(B)$, determined by the procedure described in the text. The open circles denote the upper critical field determined by transport measurements [13]. The solid lines are the theoretical phase boundaries. The dashed line is the calculated Neel temperature of the Q_A phase had the metal stayed in the normal state. The thin line labeled $B_{c2}^0(T)$ is the estimated upper critical field if the magnetic subsystem is neglected.

Concurrently with the appearance of the field-induced peaks the intensity of the zero-field magnetic reflections with scattering vector Q_F decreases and finally vanishes at 1.4 T and 100 mK. Between 0.9 and 1.4 T the magnetic structures at Q_F and Q_A coexist. The length of Q_F does not change for applied magnetic fields up to 0.9 T. Above 0.9 T a small reduction of $|Q_F|$ is observed, simultaneously with the appearance of the field-induced magnetic reflection at Q_A . The reduction is at the most 3%, just before the peaks vanish at 1.4 T.

In the main body of Fig. 1 we show the temperature dependence of the integrated intensity of the field-induced magnetic reflections for three different values of the applied fields. This shows that the intensity of the peaks increases with increasing field at a constant temperature. The results at the different values of the field show qualitatively the same temperature dependence, a rapid linear decrease when the temperature is above 0.5 K and a

cross-over into a long tail at about 2 K. At the maximum field of 1.8 T the tail extends up to a temperature of four times the zero-field value of T_N . For each value of the field $T_N(B)$ is defined as the extrapolation to zero of the linear part of the integrated intensity, as shown in the figure for the case of 1.8 T. The experimental data are summarized in the phase diagram in Fig. 2.

The theoretical phase diagram is calculated using the following parameters: 1) The crystal-field Hamiltonian of the Tm ions determined from experiments [14,15]. 2) A phenomenological RKKY interaction $J(q)$ with two parameters $J(Q_F)$ and $J(Q_A)$. The normal-state value of $J(0) = J(Q_F)$. 3) Abrikosov's formula [16] for the condensation energy of the superconducting state

$$F_s - F_n = -\frac{1}{2} B_i^2 g^2 [1.16 - 8(2^2 - 1)]^{-1}; \quad (1)$$

where B_i is the internal magnetic field, corrected for the uniform magnetization and demagnetization effects. In the present system B_i is about 10% larger than the applied field. $B_{c2}^0(T)$ is the upper critical field if the coupling to the magnetic electrons is neglected. Its dependence on $T = T_c$ is assumed to be the same as observed in the non-magnetic Lu borocarbide [17]. $B_{c2}^0(T = 0)$ has been used as a fitting parameter, and its initial value of 6.5 T (corresponding to $\mu_0 H_c = 71$ A) is close to that obtained when scaling the values of $B_{c2}^0(0)$ in the non-magnetic Lu and Y borocarbides with T_c . The other fitting parameter in Eq. (1) is the (renormalized) value of χ which is found to be 6.3, close to that determined experimentally by Cho et al. [11]. 4) The coupling between the magnetic system and the superconducting electrons is described by two parameters: a) The Anderson-Suhl reduction of $J(0)$ in the superconducting phase at zero temperature, which is found to be close to the value of $J(0)$ itself. The thermally excited quasiparticles implies that the reduction is smaller at finite temperatures. This effect is included in the calculations. b) The suppression of the superconductivity, which is assumed to be due to the superzone energy gaps near the Fermi surface produced by the magnetic ordering at Q_A . The density of states at the Fermi surface is reduced proportionally to the sizes of the energy gaps, which by themselves are proportional to the amplitude of the magnetic modulation [18]. The reduction of the density of states causes a decrease of $B_{c2}^0(T)$ in Eq. (1), which is estimated to be at most 40%.

The model calculations account reasonably well for the experimental phase boundaries in Fig. 2, and equally well for the phase diagram when the field is applied in the c direction, as measured by Eskildsen et al. [7]. The large anisotropy between the experimental upper critical field along the a and along the c axis is not an internal property of the superconducting electron system, but is due to the large difference between the magnetic a- and c-axis susceptibility of the Tm ions. Although the transformation of the Q_F state into the c-axis ferromagnet did not occur, it is clear that the Anderson-Suhl

mechanism plays an important role for the behavior of $\text{TmNi}_2\text{B}_2\text{C}$, see also the discussion by Kulic et al. [19]. The loss in the superconducting condensation energy at the field-induced transition to the normal state is compensated for by the gain in the RKKY exchange energy deriving from the uniform magnetization because of the sudden increase of $J(0)$. This mechanism explains the large reduction of the upper critical field shown in Fig. 2, and the even larger reduction in the c -axis phase diagram. Most significantly, it explains why the Q_F state is stable up to a field of 1 T applied along the c axis, i.e. as long as the system stays superconducting. In case of a normal behavior of $J(q)$, the c -axis field would destroy this phase almost immediately.

Against intuition, the short wavelength magnetic modulation in the Q_A phase affects the superconductivity state much more strongly than the long wavelength Q_F -modulation, but it should be noticed that the wavelengths of the two structures are both much shorter than λ_F . The model predicts that in a normal magnetic system the Q_A phase would be the stable one at low temperatures and fields. However, the superzone energy gaps produced by the Q_A -modulation disturb the nesting features of the Fermi surface close to this wave vector, causing a strong suppression of the superconductivity in the Tm system. This effect is also found in the measurements on e.g. Ho based borocarbides, where superconductivity is suppressed when the magnetic system enters the $Q = (0.55; 0; 0)$ phase and is regained when the system leaves this phase at a yet lower temperature [20]. Er borocarbide is the only one where the $(0.55; 0; 0)$ -phase does not seem to strain the superconducting properties severely, although the upper critical field [12] shows similarities with the observations in the Tm system. The reason that the Q_F phase does not appear in, for instance, the Er system may simply be that the RKKY interaction, being proportional to $(g-1)J^2$, is stronger in Er than in Tm making the energy difference between the two different magnetic phases too large in comparison with the superconducting condensation energy.

Improvement of the present theory is planned in order to account for the inhomogeneities in the superconducting order parameter due to the flux lines. It is difficult to understand how the low-intensity long tail of the Q_A reflections may extend up to a temperature which is twice the estimated transition temperature of the Q_A -phase in a normal system (the dashed line in Fig. 2). The phase may survive within the normal core of the flux lines, but not very far above the normal-phase transition temperature. Further experiments are planned at higher fields in order to test the theoretical predictions, e.g. that $T_N(B)$ coincides with the maximum in the in-plane upper critical field, to investigate in more detail the magnetic scattering in the long-tail regime, and to search for the Q_A -phase in the c -axis phase diagram.

In this letter we have proposed that the long wave-

length magnetic structure of $\text{TmNi}_2\text{B}_2\text{C}$ below 1.5 K owes its very existence to the fact that the material is superconducting. This was shown experimentally by applying an in-plane magnetic field, which in this Ising-like system primarily affects the superconducting state. We have found that the magnetic system enters a new phase at a critical field of 0.9 T where the order is at short wavelength, $Q_A = (0.48; 0; 0)$. We have presented theoretical calculations showing that the interplay between superconductivity and magnetism in the borocarbides is governed by two mechanisms: 1) a suppression of the ferromagnetic component of the RKKY exchange interaction in the superconducting phase, and 2) a reduction of the superconducting condensation energy from the periodic modulation of the moments at the wave vector Q_A .

We thank D. G. Naugle and K. D. D. Rathnayaka for sharing their data prior to publication. This work is supported by the Danish Technical Research Council and the Danish Energy Agency. P. C. C. is supported by the Director of Energy Research, Office of Basic Energy Science under contract W-7405-Eng-82.

Present address: DPMC, Université de Genève, 24, Quai E.-Ansermet, CH-1211 Genève 4, Switzerland.

- [1] R. N. Nagaraajan et al., Phys. Rev. Lett. 72, 274 (1994).
- [2] R. J. Cava et al., Nature 367, 252 (1994).
- [3] T. Siegrist et al., Nature 367, 254 (1994).
- [4] R. Movshovich et al., Physica C 230, 381 (1994).
- [5] J. W. Lynn et al., Phys. Rev. B 55, 6584 (1997).
- [6] B. Stemlieb et al., J. Appl. Phys. 81, 4937 (1997).
- [7] M. R. Eskildsen et al., Nature 393, 242 (1998).
- [8] J. Y. Rhee, X. Wang, and B. N. Harmon, Phys. Rev. B 51, 15585 (1995).
- [9] S. B. Dugdale et al., Phys. Rev. Lett. 83, 4824 (1999).
- [10] P. W. Anderson and H. Suhl, Phys. Rev. 116, 898 (1959).
- [11] B. K. Cho et al., Phys. Rev. B 52, 3676 (1995).
- [12] B. K. Cho et al., Phys. Rev. B 52, 3684 (1995).
- [13] D. G. Naugle, K. D. D. Rathnayaka, K. C. Lark, and P. C. Canfield, Int. J. Mod. Phys. B (to be published).
- [14] U. Gasser et al., Z. Phys. B 101, 345 (1996).
- [15] J. Jensen and A. R. Mackintosh, Rare Earth Magnetism: Structures and Excitations (Clarendon Press, Oxford, 1991).
- [16] M. Tinkham, Introduction to superconductivity (McGraw-Hill, New York, 1996) 2. edition, p. 160.
- [17] S. V. Shulga et al., Phys. Rev. Lett. 80, 1730 (1998).
- [18] R. J. Elliott and F. A. Wedgwood, Proc. Phys. Soc. 81, 846 (1963).
- [19] M. L. Kulic, A. I. Buzdin and L. N. Bulaeviskii, Phys. Lett. A 235, 285 (1997).
- [20] H. Schmidt and H. F. Braun, Phys. Rev. B 55, 8497 (1997).